

participate with sterols in the formation of membrane microdomains or lipid rafts, which are critically dependent on the sphingolipid chirality [3]. From the pharmacological side, some sphingosines display strong chirality-dependent antiproliferative properties and can be used as antitumor or cytotoxic compounds, exploiting their role in cell proliferation, migration and apoptosis [4]. Phytosphingosines form a sub-class of sphingoid bases (1, Fig. 1), most commonly consisting of a 1,3,4-trihydroxy-2-amino head and an 18-carbon aliphatic chain, like *D*-ribo-phytosphingosine (2). Some unusual phytosphingosines derivatives from marine organisms, like jaspine A (3) and jaspine B (4), have important pharmacological properties. Jaspine B (pachastrissamine), isolated from the sponges *Pachastrissa* sp. [5] and *Jaspis* sp. [6] in 2002, is biosynthesized from *D*-ribo-phytosphingosine 2 by intramolecular nucleophilic displacement and possesses a unique all-*syn* (2*S*,3*S*,4*S*)-trisubstituted tetrahydrofuran ring core. Jaspine B inhibits the ceramide and sphingomyelin synthases and shows remarkable antitumor properties on several human cancer cell lines [7–9].

Since sphingoid bases acquire biological functions with specific stereochemical configurations, interest has grown in the synthesis and biological assessment of jaspine stereoisomers [10,11] and derivatives [12]. Here we address the correlation between stereochemistry, ring-puckering and the intra- and inter-molecular interactions of jaspine B and its monohydrates from a molecular point of view, probing the isolated molecule in the cooled and collisionless environment of a supersonic jet expansion. Gas-phase studies benefit from disaggregation [13], rendering intrinsic single-molecule properties directly comparable to the *in vacuo* molecular orbital computations. This information may help the rational design of new drugs based on the jaspine skeleton. However, the 14-carbon aliphatic chain of jaspine B would create a myriad of competing conformations, impeding a high-resolution spectroscopic study. For this reason, we first prepared a specially truncated jaspine B with a shortened side chain, where we can capture the conformational and structural properties of the bioactive polar headgroup and its relation to the side chain using high-resolution rotational spectroscopy. Following chemical and spectroscopic considerations, we synthesized the 3-carbon aliphatic chain jaspine analogue of (2*S*,3*S*,4*S*)-4-amino-2-propyltetrahydrofuran-3-ol, denoted jaspine B3 (5).

Jaspine B3 is expected to display a rich three-level-deep isomerism arising from the flexible tetrahydrofuran ring, the presence of two polar amino and alcohol groups in adjacent ring atoms and the aliphatic side chain. The tetrahydrofuran five-membered ring is a common scaffold in biological compounds like nucleic acids, displaying unique torsional characteristics. The facile interconversion between twisted and envelope forms may be described as a monodimensional large-amplitude motion or pseudorotation [14], in which bent/twist puckering rotates around the ring avoiding planar configurations. Puckering can be very sensitive to ring substituents or hydration and may determine macromolecular arrangements [15–17], as in the different puckering of DNA/RNA A or B chains. Precise determination of the puckering characteristics is thus necessary to specify the pseudorotation pathways, to compare with related biomolecules or clusters and to assess the influence of the polar and aliphatic groups in the preferred structures of jaspine B. In addition, the amino and alcohol adjacent groups offer several options for intra and inter-molecular hydrogen bonding, such as O-H...N or N-H...O [15,18]. The aliphatic side chain, even truncated here to 3 carbons, adds several three-fold rotors which may engage with the ring or the polar groups creating multiple isomers.

The microsolvation of jaspine B uses one water molecule to probe the strength of the intramolecular forces in the monomer and the possibility of water to modulate molecular conformations or hydrogen bonding in the isolated molecule [13,15,19]. Specifically, water may either add or disrupt the monomer intramolecular hydrogen bonding or puckering, offering clues on the strength and nature of the intermolecular interactions [20]. All these factors make jaspine B3 a testbed to examine the relation between intra- and inter-molecular interactions and conformation in sphingosine headgroups and to relate to biomolecular interactions. The present work extends previous gas-phase structural studies on mimics of sphingoid headgroups, restricted to small 3- or 4-carbon open-chain amino-alcohols like serinol [21] or the threoinol [22] and allo-threoinol [23] diastereoisomers. These studies have detected multiple low-energy isomers where intramolecular hydrogen bonds may produce linear or cyclic networks of hydrogen bonds, revealing initial connections between chirality and intramolecular interactions. The investigation of jaspine B3 represents a qualitative leap in the progress toward molecular studies of larger SLs.

The spectroscopic work used advanced chirped-pulse broadband microwave spectroscopy [24], offering much higher resolu-

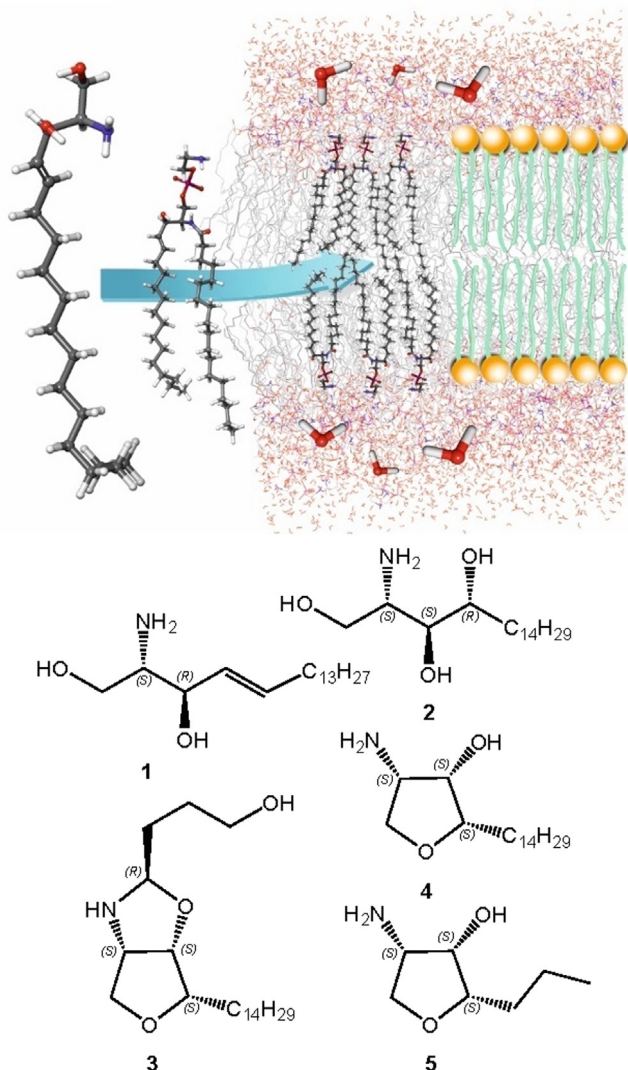


Fig. 1. Upper panel: Schematics of the insertion of sphingosine into sphingomyelin and into a (simplified) lipidic bilayer. Lower panel: Molecular formulas of sphingosine (1), *D*-ribo-phytosphingosine (2), jaspine A (3), jaspine B (4) and jaspine B3 (5).

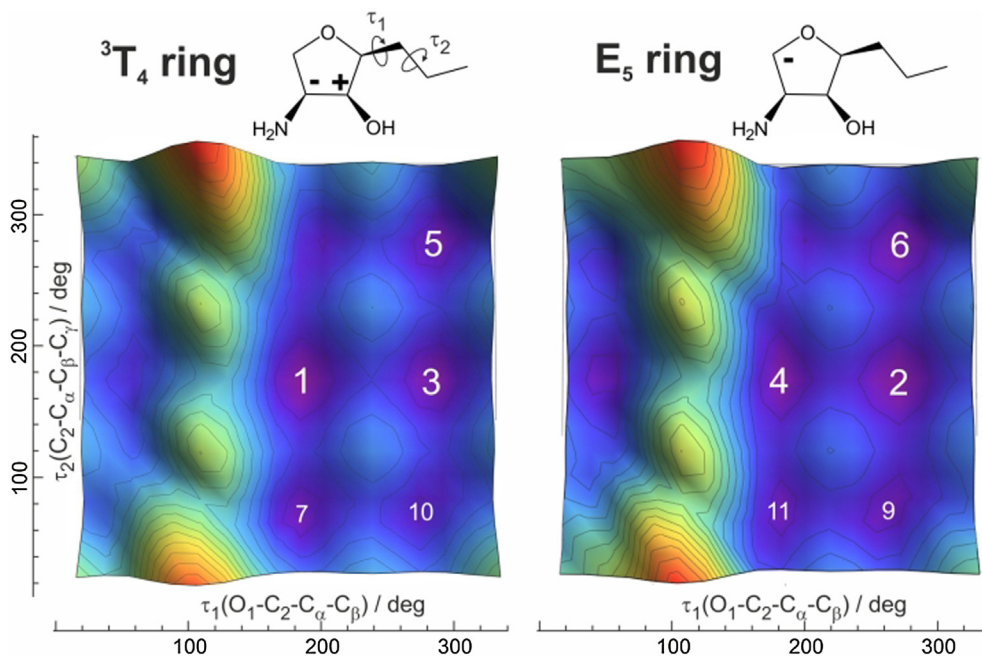


Fig. 4. PES scans of the sidechain for the 3T_4 and E_5 ring conformations, showing the location of the most stable conformers. The sidechain behavior is similar for both 3T_4 and E_5 puckering conformations, with preference for G- and A orientations (numerical values in Supporting Information). In this blue-to-red color scheme the smaller energies are dark blue. The isomer locations are marked 1-11.

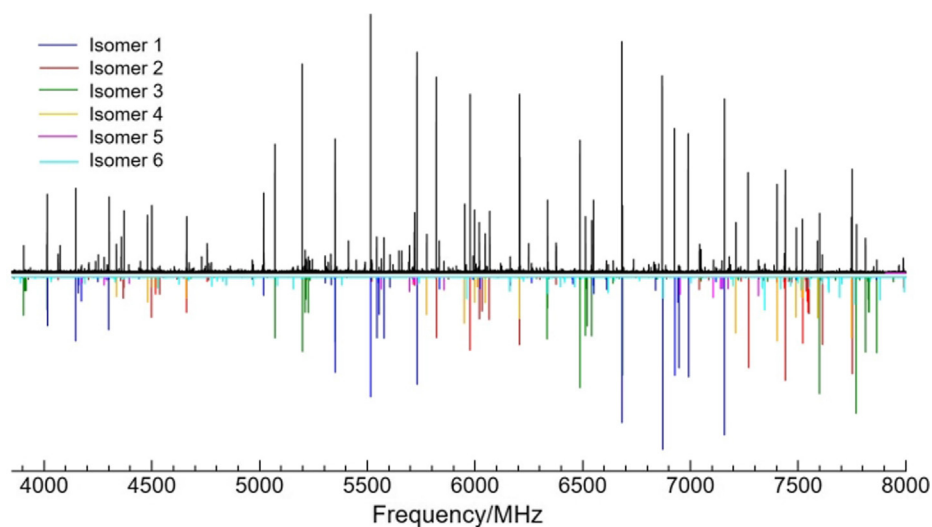


Fig. 5. A 4 GHz section of the jet-cooled microwave spectrum of Jaspine B3. Upper trace: Experimental spectrum; Lower trace: Fit of the different conformers 1-6 using the rotational parameters of Table 1 and a rotational temperature of 2 K.

second-order *ab initio* perturbation theory [30] (MP2) and the same basis set. Vibrational frequency calculations provided a harmonic force field, centrifugal distortion and zero-point energy corrections. For the dimer, complexation energies were corrected for basis-set superposition errors with the counterpoise method [31].

3. Results and discussion

3.1. Potential energy surface

The investigation of jaspine B3 started with a description of the potential energy surface (PES). The computational results are summarized in Tables S1-S3 (monomer) and S4-S5 (monohydrate, Supporting Information). The calculations suggested a rich

conformational landscape, generating up to 52 conformers for the monomer and 212 isomers for the monohydrate within 25 kJ mol⁻¹.

The conformational landscape of jaspine B3 can be categorized using the ring conformation and the side chain orientation (dihedrals $\tau_1 = O1C2-C\alpha-C\beta$, $\tau_2 = C2C\alpha-C\beta C\gamma$ in Scheme S1). The conformational maps in Fig. 2 and S1-S2 (Supporting Information) and the puckering diagram of Fig. 3 specify ring puckering using the Cremer-Pople (CP) curvilinear coordinates [32], allowing precise comparisons with related five-membered dominant ring geometries, either twisted 3T_4 (conformers 1, 3, 5, 7, 10, 13) or envelope E_5 (conformers 2, 4, 6, 9, 11, 15), both with the alcohol pointing to the amino group. Three higher-energy isomers show a different 3T_2 (8, 12) or 3T_4 (14) twist conformation, with the amino group

Table 1

Experimental rotational parameters of the six observed isomers of jaspine B3 and the dimer (jaspine B3)-water. See Supporting Information for theoretical values.

System	Jaspine B3						Jaspine B3-water W2
Isomer	1	2	3	4	5	6	
Puckering	3T_4	E_5	3T_4	E_5	3T_4	E_5	3T_4
Side chain	AA	G-A	G-A	AA	G-G ⁻	G-G ⁻	AA
A / MHz ^a	2795.4709(11) ^c	2243.8144(10)	3174.6108(18)	2462.18(14)	2901.8114(71)	2298.2034(14)	1382.331(28)
B / MHz	741.10679(29)	801.63564(35)	686.67666(33)	804.3406(12)	750.5540(14)	857.91008(53)	667.2511(10)
C / MHz	645.70568(22)	704.55488(32)	616.73418(28)	696.1520(11)	677.8354(14)	743.21068(50)	485.6647(10)
3/2 χ_{aa}	1.569(16)	2.2950(97)	3.090(17)	0.392(52)	4.04(13)	2.897(35)	3.355(47)
1/4 ($\chi_{bb}-\chi_{cc}$)	0.3322(51)	-1.7099(27)	-0.2650(49)	-1.314(13)	-0.585(32)	-1.6560(90)	-0.893(40)
D_J / kHz	[0.0] ^d	0.1626(66)	[0.0]	[0.0]	[0.0]	0.3314(62)	[0.0]
D_{JK} / kHz	[0.0]	-0.754(11)	[0.0]	[0.0]	[0.0]	[0.0]	[0.0]
D_K / kHz	[0.0]	3.24(13)	[0.0]	[0.0]	[0.0]	[0.0]	[0.0]
$ \mu_a $ / D	+++ ^e	+++	+++	+++	++	+	+++
$ \mu_b $ / D	+	++	+	-	-	++	-
$ \mu_c $ / D	++	+	++	-	-	-	-
N^b	161	168	103	62	36	56	45
σ / kHz	15.2	10.2	13.4	12.5	13.5	15.7	12.4

^a Rotational constants (A, B, C), nuclear quadrupole coupling parameters (χ_a, χ_b, χ_c), Watson's S-reduction centrifugal distortion constants (D_J, D_{JK}, D_K ; the constants d_1 and d_2 were fixed to zero) and electric dipole moments ($\mu_x, \alpha = a, b, c$). ^bNumber of fitted transitions (N) and rms deviation (σ) of the fit. ^cStandard errors in parentheses units of the last digit. ^dValues in square brackets were fixed to zero. ^eOne or more positive signs indicates the observation and intensity of the corresponding transitions.

towards the alcohol. For each geometry several side-chain orientations are possible. Additional bidimensional PES scans for the 3T_4 and E_5 ring conformations in Fig. 4 used B3LYP-D3(BJ) and show preference for atoms C β and C γ to be oriented either *antiperiplanar* (A, $\tau_1 \approx 180^\circ$) or *gauche*- (G-, $\tau_1 \approx 300^\circ$) respect to the ring heteroatom, with relatively small energy differences between the lowest-lying conformers and close similarity between the 3T_4 and E_5 ring conformations.

3.2. Jaspine B3 monomer

The computational predictions were assessed in our spectroscopy experiment. The dense rotational spectrum in Fig. 5 immediately suggested the presence of multiple competing isomers. The spectrum was then searched iteratively using simulations with the trial rotational constants in Tables S1 (B3LYP), S2 (B2PLYP) and S3 (MP2) in the Supporting Information. Most transitions exhibited small (<1 MHz) nuclear quadrupole coupling effects (Figures S3-S4, Supporting Information), so the spectrum was analyzed with a Watson's semirigid-rotor Hamiltonian with quadrupole terms appropriate for the ${}^{14}\text{N}$ nucleus (nuclear spin $I = 1$) [33]. Both the global spectral patterns and the individual hyperfine effects were extremely sensitive to molecular geometry, leading to an unambiguous structural identification. The process was repeated iteratively and finally a total of six different conformers were positively identified, with the experimental parameters and measured transitions presented in Table 1 and S6-S12 (Supporting Information). The comparison of experiment and theory confirmed the detection of all six jaspine B3 isomers with conformational energies below 3 kJ mol⁻¹ (outlined in Fig. 2). Differences between the experimental and theoretical rotational constants were below 0.8% for B3LYP and B2PLYP, while MP2 offered worse results (<2.8%). Relative intensities on a common set of μ_a transitions gave estimations for the jet populations of 2:1:3:4:6:5 = 1.0 > 0.69(6) > 0.34(3) \approx 0.34(3) > 0.09(1) > 0.06(1), indicating that isomer 2 is the most populated. However, population ratios cannot be translated into energy differences as conformational relaxation is often observed in the jet in case of low (<5–10 kJ mol⁻¹) interconversion barriers [34,35]. We explored plausible conversions between non-observed and detected species in Figures S5-S8 (Supporting Information), obtaining barriers in the range 6.9–17.3 kJ mol⁻¹ even for changes limited to the side chain orientation. The smaller barriers exchanging conformers 10 and 3 or 9 and 2 (6.9 and 7.1 kJ mol⁻¹, respectively) may be surmountable in the jet, explaining the absence of additional specific isomers.

The experimentally observed isomers of jaspine B3 comprise three 3T_4 twist (1, 3, 5) and three E_5 envelope (2, 4, 6) conformations. Topological analyses of the reduced electronic density with NCI plots [36] in Figures S9-S10 (Supporting Information) and the structural data in Tables S13-S18 (Supporting Information) confirmed the presence of intramolecular hydrogen bonds in all

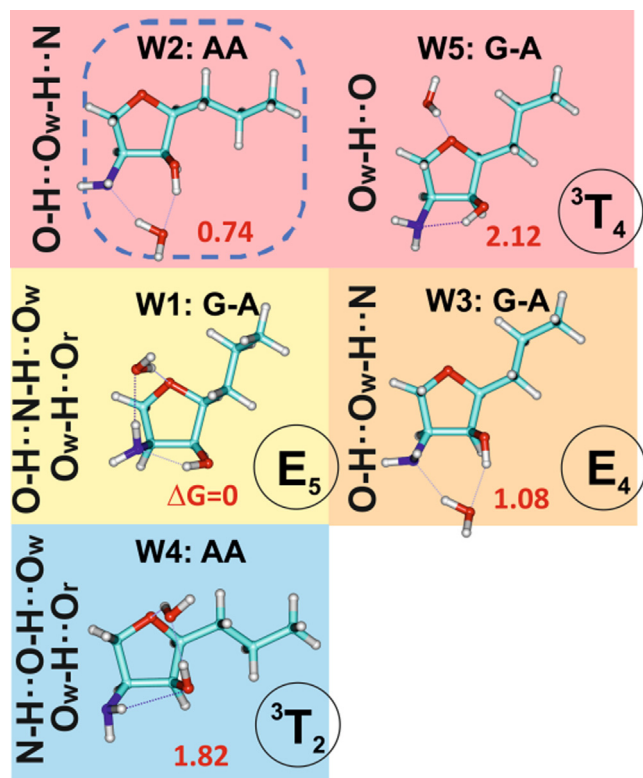


Fig. 6. Conformational landscape of the most stable (jaspine B3)-water monohydrates W1 to W5 (T = twist, E = envelope), with predicted free energies at 1 atm and 298 K (B3LYP-D3, kJ mol⁻¹; see Supporting Information for B2PLYP and MP2 values). The observed species is encircled.

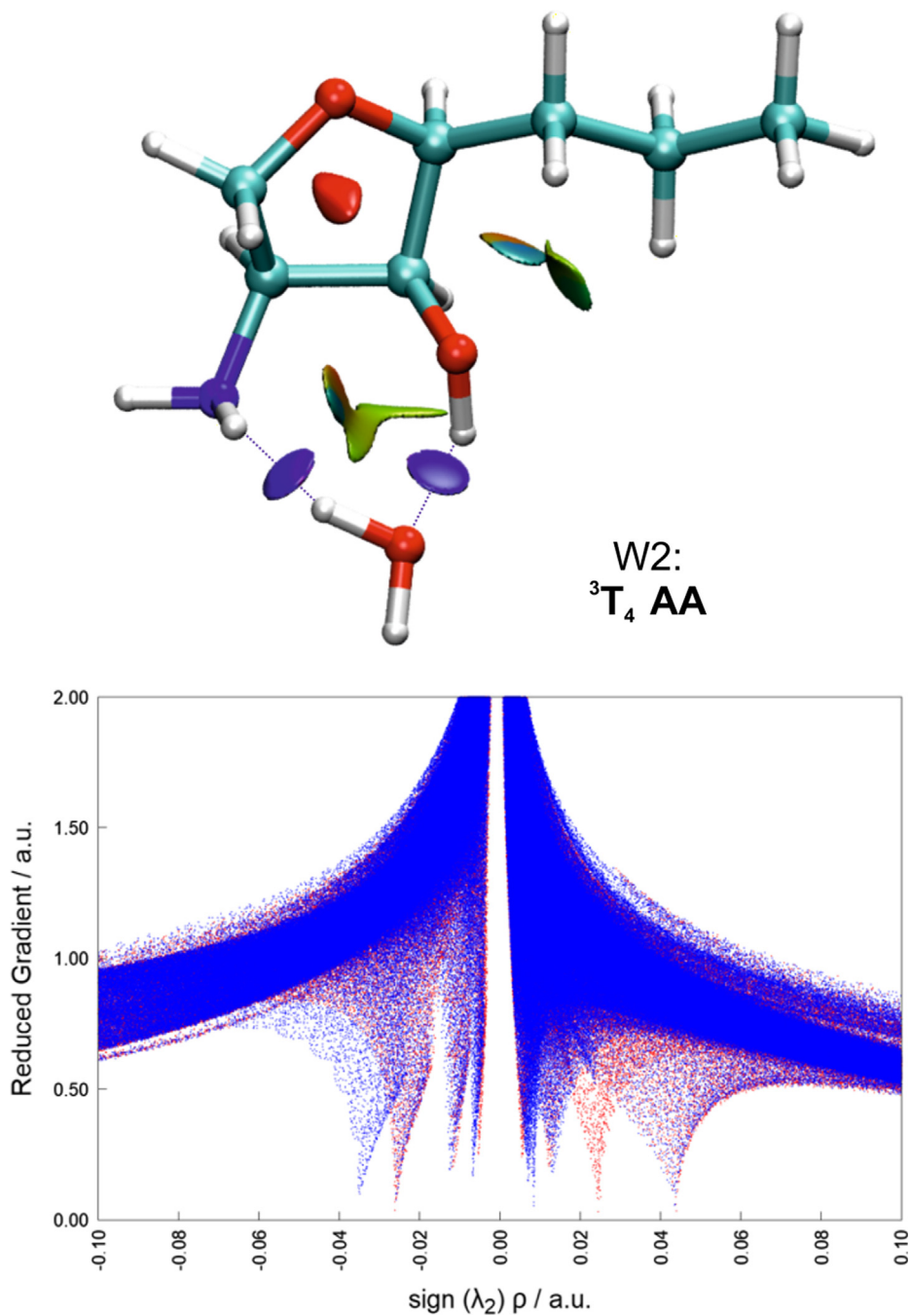


Fig. 7. Upper panel: NCI plot mapping the inter- and intramolecular interactions in the observed monohydrate of jaspine B3. The blue and green shades indicate strongly and weakly attractive interactions, respectively (see Supporting Information), characterizing the hydrogen bonds. Lower panel: Plot of the reduced electronic density gradient s ($= \frac{1}{2(3\pi^2)^{1/3}} \frac{|\nabla \rho|}{\rho^{4/3}}$) vs. the signed electronic density comparing conformer 1 ($= {}^3T_4$ AA, red trace) and the water dimer W2 ($= {}^3T_4$ AA, blue trace). Attractive critical points are shown as negative minima of the curve (see Supporting Information). The comparison shows the formation of new interactions in the dimer. (For interpretation of the references to colour in this figure legend, the reader is referred to the web version of this article.)

isomers. The twisted 3T_4 isomers display a single O-H...N hydrogen bond, as this ring conformation increases the distance between the amino group and the ring oxygen (B3LYP: $r(\text{O-H}\cdots\text{N}) = 2.07 \text{ \AA}$). Conversely, the E_5 conformers may establish a network of two consecutive O-H...N-H...O_{ring} hydrogen bonds, since the ring permits a closer approach of one of the amino N-H bonds towards the ring heteroatom. These isomers combine a relatively short O-H...N hydrogen bond ($r(\text{O-H}\cdots\text{N}) = 1.94\text{--}1.99 \text{ \AA}$) with a long N-H...O_{ring} contact ($r(\text{N-H}\cdots\text{O}_{\text{ring}}) = 2.59\text{--}2.61 \text{ \AA}$). All intramolecular interactions are constrained by the ring geometry but fall within the statistical bounds for these hydrogen bonds [15,18].

3.3. Jaspine B3 monohydrate

The addition of water to the carrier gas line permitted the observation of new transitions from the monohydrated dimer (Table S19, Supporting Information). Figure S11 (Supporting Information) shows the nuclear quadrupole coupling hyperfine effects of some typical rotational transitions, which were well reproduced with a semirigid-rotor model. The experimental results in Table 1 and Table S20 (Supporting Information) can be compared with calculations of the conformational landscape in Tables S4 (B3LYP) and S5 (B2PLYP and MP2, Supporting Information), which predicted

thirteen different isomers below 5 kJ mol⁻¹. The experimental data unequivocally correspond to isomer W2 of Fig. 6-7 and Figure S12 (Supporting Information), associated to a ³T₄ ring puckering conformation. A few transitions were tentatively assigned to isomer W1, but the small dataset did not permit a definitive confirmation. Consistently, the W2 monohydrate shows the largest complexation energy (B2PLYP: -49.5 kJ mol⁻¹). The observed W2 monohydrate can be rationalized as result of the insertion of a water molecule in between the alcohol and amino groups of the monomer ³T₄ global minimum, also predicted for isomer W3 (E₄). Conversely, isomers W1, W4 and W5 would correspond to a common pattern of addition to the ring oxygen for three different puckerings. The puckering plot of Fig. 3 evidences small ring distortions of isomer W2 respect to the monomer, so the water role is to reinforce the characteristic network of hydrogen bonds in which water always participates simultaneously as proton donor and acceptor. NCI plots in Fig. 7 and structural data in Table S21 (Supporting Information) confirmed the complementarity and formation of new intra- and intermolecular interactions in the dimer. The ³T₄ dimer exhibits two characteristic O-H...O_w-H...N-H hydrogen bonds, while other hydrates may show up to three consecutive O-H...N-H...O_w-H...O_r hydrogen bonds. The addition of water to the ring oxygen gives the shortest hydrogen bond (B3LYP: $r(\text{O}_w\text{-H}\cdots\text{O}_r) = 1.83\text{--}1.85 \text{ \AA}$). Water also behaves as proton donor to the amino group when inserting in between the polar groups in the ring ($r(\text{O}_w\text{-H}\cdots\text{N}) = 1.90 \text{ \AA}$), confirming the amino group as better hydrogen bond acceptor and poorer donor, as observed in serinol [21] and threoninol [22,23].

4. Conclusion

The observation of six isomers and the most stable monohydrate of jaspine B3 provides an accurate description of the conformational landscape and microsolvation properties. As observed in other biomolecules with a tetrahydrofuran core, in particular nucleotides, ring puckering turns fundamental, as relatively small puckering differences are amplified by the ring substituents, conditioning intermolecular interactions and large-scale molecular behaviour [15]. Puckering preferences are relatively unchanged for the monomer and hydrates and specifically dependent on the ring substituents, as observed in furanosides [37]. This result confirms previous observations that molecular stability arises from an interplay of intrinsic hyperconjugative electronic effects and intramolecular interactions [16,17]. Similarities in the side chain for different puckering conformations suggest a secondary role of the aliphatic group, as in amino acids [38]. As a result, the specific jaspine stereochemistry, which locates the polar groups on the same side of the ring, is determinant of its intra- and intermolecular interactions, creating a double-faced molecule where the exposed lone-pair electrons on the substituents face may easily catalyze the formation of intermolecular aggregates. The microsolvation of jaspine B3 shows multiple hydration patterns by proton donation to the oxygen ring or the amino group, creating chirality-dependent hydrogen bond networks familiar in sugar hydration [39,40], which may be instrumental for the jaspine biological role. Finally, the importance of gas-phase molecular studies to complement crystal diffraction or liquid NMR information of biochemical building blocks should be outlined, marking future routes to integrated studies covering from the bare molecule to the integration of biomolecular units in the hydrated biological environment.

CRedit authorship contribution statement

Rizalina T. Saragi: Validation, Formal analysis, Investigation, Data curation, Writing – original draft, Writing – review & editing,

Visualization. **Marcos Juanes:** Validation, Investigation, Writing – review & editing. **José L. Abad:** Conceptualization, Methodology, Resources, Investigation, Writing – review & editing. **Ruth Pina-cho:** Software, Resources, Writing – review & editing. **José E. Rubio:** Software, Resources, Writing – review & editing. **Alberto Lesarri:** Conceptualization, Methodology, Resources, Data curation, Writing – original draft, Writing – review & editing, Supervision, Project administration, Funding acquisition.

Declaration of Competing Interest

The authors declare that they have no known competing financial interests or personal relationships that could have appeared to influence the work reported in this paper.

Acknowledgements

Funding support from the Spanish MICINN-FEDER (grant PGC2018-098561-B-C22) is gratefully acknowledged. M.J. and R.T.S. are thankful for predoctoral contracts from the MICINN and UVA, respectively.

Appendix A. Supplementary material

Supplementary data to this article can be found online at <https://doi.org/10.1016/j.saa.2021.120531>.

References

- [1] B. Cinque, L. Di Marzio, C. Centi, C. Di Rocco, C. Riccardi, M.G. Cifone, Sphingolipids and the immune system, *Pharmacol. Res.* 47 (2003) 421–437, [https://doi.org/10.1016/S1043-6618\(03\)00051-3](https://doi.org/10.1016/S1043-6618(03)00051-3).
- [2] T. Ariga, W.D. Jarvis, R.K. Yu, Role of sphingolipid-mediated cell death in neurodegenerative diseases, *J. Lipid Res.* 39 (1) (1998) 1–16, [https://doi.org/10.1016/S0022-2275\(20\)34198-5](https://doi.org/10.1016/S0022-2275(20)34198-5).
- [3] K. Simons, E. Ikonen, Functional rafts in cell membranes, *Nature*. 387 (6633) (1997) 569–572.
- [4] J. Padrón, Sphingolipids in Anticancer Therapy, *Curr. Med. Chem.* 13 (2006) 755–770, <https://doi.org/10.2174/092986706776055553>.
- [5] I. Kuroda, M. Musman, I.I. Ohtani, T. Ichiba, J. Tanaka, D.G. Gravalos, T. Higa, Pachastrissamine, a cytotoxic anhydrophytosphingosine from a marine sponge, *Pachastrissa* sp., *J. Nat. Prod.* 65 (10) (2002) 1505–1506, <https://doi.org/10.1021/np010659y>.
- [6] V. Ledroit, C. Debitus, C. Lavaud, G. Massiot, Jaspines A and B: two new cytotoxic sphingosine derivatives from the marine sponge *Jaspis* sp., *Tetrahedron Lett.* 44 (2) (2003) 225–228, [https://doi.org/10.1016/S0040-4039\(02\)02541-8](https://doi.org/10.1016/S0040-4039(02)02541-8).
- [7] F. Cingolani, F. Simbari, J.L. Abad, M. Casasampere, G. Fabrias, A.H. Futerman, J. Casas, Jaspine B induces nonapoptotic cell death in gastric cancer cells independently of its inhibition of ceramide synthase, *J. Lipid Res.* 58 (8) (2017) 1500–1513, <https://doi.org/10.1194/jlr.M072611>.
- [8] Y. Yoshimitsu, S. Oishi, J. Miyagaki, S. Inuki, H. Ohno, N. Fujii, Pachastrissamine (jaspine B) and its stereoisomers inhibit sphingosine kinases and atypical protein kinase C, *Bioorg. Med. Chem.* 19 (18) (2011) 5402–5408, <https://doi.org/10.1016/j.bmc.2011.07.061>.
- [9] Y. Salma, E. Lafont, N. Theriville, S. Carpentier, M.-J. Bonnafé, T. Levade, Y. Génisson, N. Andrieu-Abadie, The natural marine anhydrophytosphingosine, Jaspine B, induces apoptosis in melanoma cells by interfering with ceramide metabolism, *Biochem. Pharmacol.* 78 (5) (2009) 477–485, <https://doi.org/10.1016/j.bcp.2009.05.002>.
- [10] D. Canals, D. Mormeneo, G. Fabriàs, A. Llebaria, J. Casas, A. Delgado, Synthesis and biological properties of Pachastrissamine (jaspine B) and diastereoisomeric jaspines, *Bioorganic, Med. Chem.* 17 (1) (2009) 235–241, <https://doi.org/10.1016/j.bmc.2008.11.026>.
- [11] M. Martinková, J. Gonda, Synthetic analogues of marine cytotoxic jaspine B and its stereoisomers, *Carbohydr. Res.* 482 (2019) 107737, <https://doi.org/10.1016/j.carres.2019.06.016>.
- [12] H. Yang, Y. Li, H. Chai, T. Yakura, B.o. Liu, Q. Yao, Synthesis and biological evaluation of 2-epi-jaspine B analogs as selective sphingosine kinase 1 inhibitors, *Bioorg. Chem.* 98 (2020) 103369, <https://doi.org/10.1016/j.bioorg.2019.103369>.
- [13] J.-P. Schermann, Spectroscopy and Modeling of Biomolecular Building Blocks, Elsevier (2008), <https://doi.org/10.1016/B978-0-444-52708-0.X5001-1>.
- [14] A.H. Mamliev, L.N. Gunderova, R.V. Galeev, Microwave spectrum and hindered pseudorotation of tetrahydrofuran, *J. Struct. Chem.* 42 (2001) 365–370, <https://doi.org/10.1023/A:1012448618502>.

